RESEARCH ARTICLE

Development and Performance Analysis of Five Phase Induction Motor

P. SRINIVASA VARMA[1], (Senior Member, IEEE), **K. P. PRASAD RAO**[2], (Member, IEEE),
C. V. RAVIKUMAR[3], **GIOVANNI PAU**[4], (Member, IEEE), **K. SATHISH**[3],
AND RAJEEV PANKAJ NELAPATI[3], (Senior Member, IEEE)

[1]Department of EEE, Koneru Lakshmaiah Education Foundation, Guntur, Andhra Pradesh 522302, India
[2]Department of EEE, Narayana Engineering College, Gudur, Andhra Pradesh 524101, India
[3]School of Electronics Engineering, Vellore Institute of Technology, Vellore, Tamil Nadu 632014, India
[4]Faculty of Engineering and Architecture, Kore University of Enna, 94100 Enna, Italy

Corresponding authors: C. V. Ravikumar (cvrkvit@gmail.com) and Giovanni Pau (giovanni.pau@unikore.it)

ABSTRACT In light of the constant need for more energy, modern society is characterized by constant technical development, especially in the field of electricity. Due to the limitations of the voltage at which it may be given, it has a finite value. Energy providers and consumers are both subject to consumption restrictions. Multiphase systems are a viable option for dealing with this issue. Multiphase systems are currently being used to tackle the issue, and progress in this area of study is swift. The importance of multiphase supply cannot be overstated in the realm of drives and other necessities. The Five Phase Induction Motor (FPIM) construction and performance analysis are discussed in this study. MATLAB/SIMULINK is used to evaluate FPIM's performance. The experimental findings of the developed FPIM are presented in this work.

INDEX TERMS Five phase induction motor, modelling, construction, operation, revolving flux, torque developed, phase loss.

I. INTRODUCTION

Numerous peer-reviewed papers have made the following observations in three to five phase converter transformers fed FPIM operation. For transforming three phases of supply into one phase of supply, phase balancers are classified as standstill and revolving balancers [1]. The 2-ph 5-wire system essential needs of service continuity, safety, security, normal voltages, flexibility, and decreased cost, among others, are primarily contrasted with the 3-Φ, 4-wire star system [2]. For various systems, electrical properties are analyzed using 60^0 reactance and corona initiation voltage [3]. Because the poles coincide due to the even number of phases, phases with odd numbers are preferable [4]. Existing single-phase loads are replaced with three phase loads [5].

In 1991, E. H. Badawy et al. presented a novel approach for 6-Φ power transmission [6]. The high order technique is used to calculate careful and reasonable faults

extremely effectively. A new topology for better torque non sine 5-us machine due to th rotor structure of synchronous reluctance machine was proposed for a specific machine. The suggested 5-Φ synchronous machine has a much higher torque density than the 3-Φ synchronous machine due to the interaction of magnetic field and armature current and the efficient usage of triplen harmonics [7], [8]. Power electronic converters power multiphase machines with more than three phases [9].

In 1974, a customized transformer has been designed [10] with different cores. The reactance of the transformer under load is investigated by adjusting the delay angle of the converter [11]. For the five limb step up 3-Φ transformer, a new electromagnetic transient analysis technique was used. Current and fluxes are analyzed in the transient mode using the electromagnetic transient programme (EMTP) [12], [13]. One of the transient analyses is the mid frequency model of an improved transformer for transient analysis. The transformer core is saturated due to geometrical induced currents and ferromagnetic resonance conditions,

The associate editor coordinating the review of this manuscript and approving it for publication was Claudia Raibulet.

and high frequency components appear in the voltage-current waveforms [14], [15].

When the FPIM with controlling mechanism is proposed, the speed must be managed in a variety of methods. Dynamic system performance was improved and it was appropriately employed for medium and low switching frequency applications using the conventional method: direct torque control of a 3-level 5-ph inverter [16], a 5-IM drive operating at low speed with an LC filter to evaluate harmonics and analyze total harmonic distortion [17], [18], and the vector control method. A 5-IM drive with DTC is utilized in artificial approaches. The elimination of harmonics and the optimal switching sequence resulted in efficient sinusoidal distributed windings of the proposed drive [19], [20], and the starting currents are time-varying utilizing fuzzy rules. The voltage drop of the switching device and the speed of the motor were used to examine a full voltage technique of the proposed drive [21]. Examples of inverter-based solutions include a 4-level IM drive with open ending for SVPWM methodology and Direct Torque Control (DTC) as an alternative to standard techniques of regulating via Pulse Width Modulation (PWM), FOC, and DTC methodologies [22], [23]. The SVPWM system with Sampled Average Zero Sequence Elimination (SAZE) is well-known for suppressing the zero-sequence voltage on average during each sample time period [24].

According to the review of studies cited above, multiphase machine drives saw very little attention from researchers until far into the 20th century. Using a multiphase transformer and power converters, this study created a multiphase machine drive to enhance reliability, efficiency, and reduce torque ripples caused by the problem of dynamic voltage sharing that arises when conventional machines are connected in shunt or series for high power applications.

In this section, the importance of five phase system and comprehensive literature survey on phase system are presented. The constructional features of FPIM are discussed in Section II. Section III presents the basic operating principle of FPIM. The modeling of PFIM is explicated in Section IV. The fabrication of proposed FPIM is presented in Section V. The simulation and experimental results are analyzed in Section VI and VII. Finally, the conclusions of the work are presented in Section VIII.

II. CONSTRUCTION OF FIVE PHASE INDUCTION MOTOR
The montage of the stator and rotor of an induction motor has been accomplished. In comparison to the conventional motor, the motor under consideration exhibits slight differences in both production and functionality. The stator of the motor under consideration has been energized with an alternating current, resulting in the production of a rotating magnetic field by the rotor. The aforementioned two pieces comprise internal components such as winding slots, core winding, centrifugal switch, end ring, and bearing. Similar to conventional motors, the rotor bars of the proposed motor were angled slightly to ensure optimal performance.

An induction motor has stator windings that have been installed in their proper stator slots. The induction motor winding is insulated to reduce core loss and boost efficiency. The Five Phase Induction Motor (FPIM) that has been proposed has twenty slots and two poles. In contrast, a standard induction motor has 24 slots and 4 poles. As a result, the cost of copper material for winding is reduced. Finally, FPIM features low core loss, great efficiency, and high reliability.

In a motor, an air gap flux existed between the stator and rotor. Once the stator winding has been energized by the alternating current source, rotating flux will be generated and circulated in the air gap. Regardless of the quantity of poles or the frequency of the supply, it remains constant. Essentially, this flux is revolving around the rotor's stationary conductors. The EMF will then be generated in the conductors of the stationary rotor.

Based on rotor construction, there are two types of IM: squirrel cage rotors and slip rings or phase wound rotors. End rings have short-circuited the rotor bars in the Squirrel Cage Rotor. The rotor bars are likewise slightly inclined. As a result, it is possible to reduce magnetic noise and overcome rotor magnetic locking. Adding external resistance to boost beginning torque is not possible due to short circuited rotor bars, however it is possible in Slip Ring (or) phase Wound Rotor. As a result, limiting beginning currents improves torque, and these types of rotors are occasionally utilised in industry. Except for the configuration of the poles, the proposed FPIM structure is the same as conventional IM. The number of poles in suggested FPIM is multiples of five, whereas in traditional it is three.

III. BASIC OPERATING PRINCIPLE OF PROPOSED FPIM
When the stator is driven by a 5-volt supply, a fixed magnitude revolving magnetic field is generated and the stator rotates at synchronous speed. The magnetic field above cuts the rotor conductor, causing emf to be induced and massive circulating currents to flow through the external low resistance rotor. At startup, the induced current frequency equals the supply frequency. Lenz's law states that induced current always moves in the opposite direction of that of its origin. As a result, the rotor starts to circle in the direction of the rotating field while attempting to retain the same speed in order to reduce the relative speed. It always spins more slowly than the rotating magnetic field, though. The standard 3-phase operational-principle is analogous to this operation.

A. ROTATING FILED PRODUCTION FOR THE PROJECTED FPIM
As previously indicated, the revolving field evolved as a result of current generation in the stator after being fed by the 5-Φ supply. Total flux can be calculated using the maximum flux instants indicated below:

$$\phi_a = \phi_m \sin(\omega t) \tag{1}$$

$$\phi_b = \phi_m \sin\left(\omega t + \frac{2\pi}{5}\right) \tag{2}$$

$$\phi_c = \phi_m \sin\left(\omega t + \frac{4\pi}{5}\right) \tag{3}$$

$$\phi_d = \phi_m \sin\left(\omega t + \frac{6\pi}{5}\right) \tag{4}$$

$$\phi_e = \phi_m \sin\left(\omega t + \frac{8\pi}{5}\right) \tag{5}$$

As can be seen from Eqns. (1) through (5), the FPIM fluxes have a 72°-phase shift, and this shift is also reflected in the stator currents that are created. The greatest flux that can be produced by a three-phase supply in a three-phase induction motor is 1.5 times the total flux that can be produced. It is different in the FPIM that has been proposed. Fig. 1 presents the results of certain in-depth analyses together with some instants. It is varied in the proposed FPIM. Detailed analyses with some instants are shown in Fig. 1.
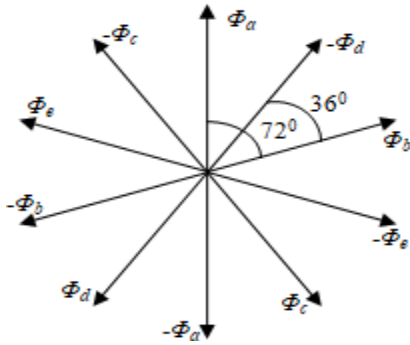
FIGURE 1. Flux generated by FPIM in five phases.
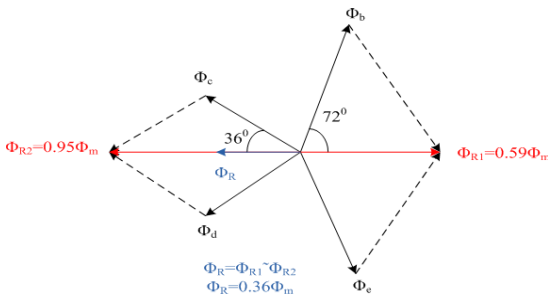
FIGURE 2. Analysis of resultant flux in mode-1.

The resultant flux, Φ_R obtained in Fig. 2 is revolving with fixed speed in the air gap of planned FPIM. This Φ_R is in terms of Φ_m has analyzed in this mode-1 from above phasor diagram.

At $\omega t = 0°$,

$$\Phi_a = 0$$
$$\Phi_b = 0.95\Phi_m$$
$$\Phi_c = 0.59\Phi_m$$
$$\Phi_d = 0.59\Phi_m$$
$$\Phi_e = 0.95\Phi_m \tag{6}$$

In next position of Φ_R is in terms of Φ_m has analyzed in this mode-2 from above phasor diagram and it is shown in Fig. 3.

At $\omega t = 72^0$,

$$\Phi_a = 0.95\Phi_m$$
$$\Phi_b = 0$$
$$\Phi_c = 0.95\Phi_m$$
$$\Phi_d = 0.59\Phi_m$$
$$\Phi_e = 0.59\Phi_m \tag{7}$$
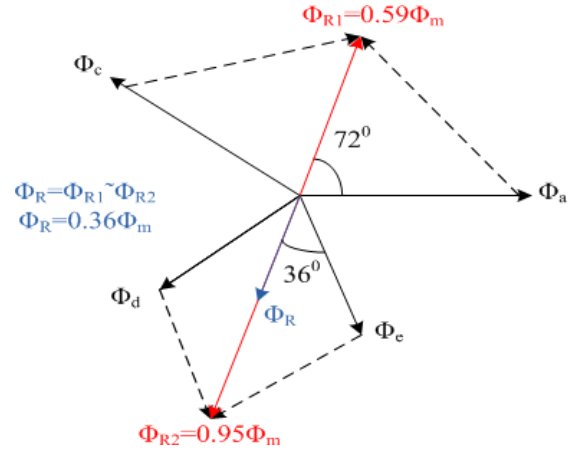
FIGURE 3. Analysis of resultant flux in mode-2.

In next position of Φ_R is in terms of Φ_m has analyzed in this mode-3 from above phasor diagram and it is shown in Fig. 4.

At $\omega t = 144°$,

$$\Phi_a = 0.59\Phi_m$$
$$\Phi_b = 0.95\Phi_m$$
$$\Phi_c = 0$$
$$\Phi_d = 0.95\Phi_m$$
$$\Phi_e = 0.59\Phi_m \tag{8}$$
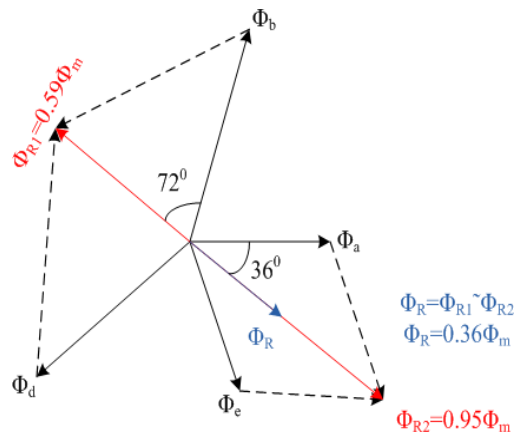
FIGURE 4. Analysis of resultant flux in mode-3.

In next position of Φ_R is in terms of Φ_m has analyzed in this mode-4 from above phasor diagram and it is shown in Fig. 5.

$$At\ \omega t = 216°,$$
$$\Phi_a = 0.59\Phi_m$$
$$\Phi_b = 0.59\Phi_m$$
$$\Phi_c = 0.95\Phi_m$$
$$\Phi_d = 0$$
$$\Phi_e = 0.95\Phi_m \tag{9}$$
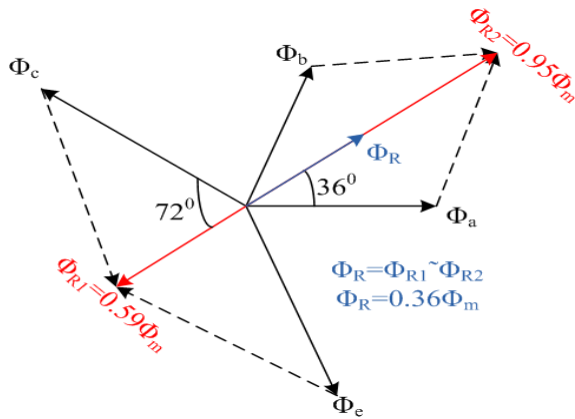
FIGURE 5. Analysis of resultant flux in mode-4.

In next position of Φ_R is in terms of Φ_m has analyzed in this mode-5 from above phasor diagram and it is shown in Fig. 6.

$$At\ \omega t = 288°,$$
$$\Phi_a = 0.95\Phi_m$$
$$\Phi_b = 0.59\Phi_m$$
$$\Phi_c = 0.59\Phi_m$$
$$\Phi_d = 0.95\Phi_m$$
$$\Phi_e = 0 \tag{10}$$

B. PRODUCTION OF TORQUE FOR THE PROPOSED FPIM
Consider conductor A in the rotor, which is positioned beneath the stator's North Pole. The field flux is developed and revolving in a clockwise direction, as shown in Fig. 7(a).

When compared to the stator, the rotor moves relative to it anticlockwise, as indicated by the dotted arrow in Fig. 7(b). It is possible to predict that the induced current will flow outward by utilising Fleming's right-hand rule. Because it will create an anticlockwise magnetic field around the conductor, the cork screw rule can be used to determine whether current is permitted to flow completely through a conductor. The two fields mentioned above are in the same area of the FPIM, and are shown in the Fig. 7(b), the two conductors combine to form the total field. The rotor is torqued clockwise, forcing it to revolve in the direction of the revolving magnetic field in Fig. 7(c), where the left side field is weaker.

IV. MODELING OF FPIM
A. LINEAR TRANSFORMATION IN ELECTRICAL MACHINE
To translate the numbers for a continuous equation without affecting the coefficients, a number of transformation techniques have been utilized in series. Usually used in ac machine analysis, the conversion turns a 3-Φ into a 2-Φ with zero sequence system.

The rotation-independent fixed coefficients are obtained using a different transformation technique. With this method, there is no similar motion between the stator and rotor coils, and the inductance becomes independent of rotation. Only the constant coefficients are present in the resulting matrix. The reference frame has fixed to stator in proposed FPIM due to uniform air gap and also fixed to rotating magnetic field.

B. AXIS TRANSFORMATION
Park's Transformation technique is used for axis transformation, and it has done to convert five-ph voltages in two-ph voltages to reduce the complexity of the analysis. Stationary five voltage axes are renewed into two phases as shown in Fig.8, these voltages are represented with the following equation (11), as shown at the bottom of the next page.

FPIM stator voltage equations under balanced condition are as follows:

$$V_a = V_m\ sin\ (\omega t) \tag{12}$$
$$V_b = V_m\ sin\left(\omega t + \frac{2\pi}{5}\right) \tag{13}$$
$$V_c = V_m\ sin\left(\omega t + \frac{4\pi}{5}\right) \tag{14}$$
$$V_d = V_m\ sin\left(\omega t + \frac{6\pi}{5}\right) \tag{15}$$
$$V_e = V_m\ sin\left(\omega t + \frac{8\pi}{5}\right) \tag{16}$$

FPIM transformed voltage equations with respect to stator side have mentioned below equation (17):

$$V_{ds} = R_s i_{ds} + \frac{d\psi_{ds}}{dt} - \omega_a\psi_{qs}$$
$$V_{qs} = R_s i_{qs} + \frac{d\psi_{qs}}{dt} - \omega_a\psi_{ds}$$
$$V_{xs} = R_s i_{xs} + \frac{d\psi_{xs}}{dt}$$
$$V_{ys} = R_s i_{ys} + \frac{d\psi_{ys}}{dt}$$
$$V_{0s} = R_s i_{0s} + \frac{d\psi_{0s}}{dt} \tag{17}$$

Similarly, rotor side transformed voltage and flux linkage equations are obtained. Transformed current equations on stator and rotor side of FPIM have mentioned below:

$$i_{ds} = \frac{\psi_{ds}[L_{lr} + L_m] - L_m\psi_{dr}}{[L_{ls}L_{lr} + L_{ls}L_m + L_{lr}L_m]}$$
$$i_{qs} = \frac{\psi_{qs}[L_{lr} + L_m] - L_m\psi_{qr}}{[L_{ls}L_{lr} + L_{ls}L_m + L_{lr}L_m]}$$
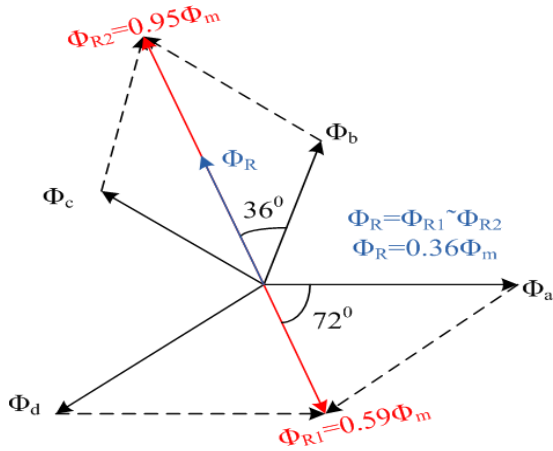
FIGURE 6. Analysis of resultant flux in mode-5.

FIGURE 7. Torque production in FPIM.

FIGURE 8. Modeling of FPIM −5-Φ to 2-Φ conversion.

$$\left[T^{-1}\right]\left[\psi_{axis}\right] = [M] \mid \left[T^{-1}\right]\left[i_{axis}\right] \tag{20}$$

$$\left[\psi_{axis}\right] = \left[TMT^{-1}\right]\left[i_{axis}\right] \tag{21}$$

$$\left[\psi_{axis}\right] = [L]\left[i_{axis}\right] \tag{22}$$

$$[L] = \left[TMT^{-1}\right] \tag{23}$$

Consequently, the following is the generalised torque equation stated in terms of the d-q axis variables.

$$T_e = \left(\frac{5}{2}\right)\left(\frac{P}{2}\right)\left(\frac{L_m}{L_m + L_{lr}}\right)\left(i_{qs}\psi_{dr} - i_{ds}\psi_{qr}\right) \tag{24}$$

The electromechanical torque produced with angular speed as given below in terms of moment of inertia (J), coefficient of dashpot (B), number of poles (P) and Load torque.

$$T_e = \left(\frac{2}{P}\right)\left(J\frac{d\omega}{dt} + B\omega_r\right) + T_L \tag{25}$$

$$T_e = PL_m\left\lfloor i_{qs}i_{dr} - i_{ds}i_{qr}\right\rfloor \tag{26}$$

$$\omega_r = \int \frac{P}{2J}\left(T_e - T_L\right)dt \tag{27}$$

Additional components x-y has used in proposed motor along with basic equations in rotor. These components have

$$i_{dr} = \frac{\psi_{dr}\left[L_{lr} + L_m\right] - L_m\psi_{ds}}{\left[L_{ls}L_{lr} + L_{ls}L_m + L_{lr}L_m\right]}$$

$$i_{qr} = \frac{\psi_{qr}\left[L_{lr} + L_m\right] - L_m\psi_{qs}}{\left[L_{ls}L_{lr} + L_{ls}L_m + L_{lr}L_m\right]}$$

$$\left[V_{axis}\right] = [T]\left[V_{phase}\right] \tag{18}$$

Equation (18) shows the axis currents and flux linkages relationship at the stator side. The transformed currents and transformed flux linkages relationship have shown in below equation (19).

$$\left\lfloor\psi_{phase}\right\rfloor = [M] \mid \left\lfloor i_{phase}\right\rfloor \tag{19}$$

$$\begin{bmatrix} V_q \\ V_d \\ V_x \\ V_y \\ V_0 \end{bmatrix} = \sqrt{\frac{2}{5}} \begin{bmatrix} \cos\theta & \cos\left(\theta + \frac{8\pi}{5}\right) & \cos\left(\theta + \frac{6\pi}{5}\right) & \cos\left(\theta + \frac{4\pi}{5}\right) & \cos\left(\theta + \frac{2\pi}{5}\right) \\ \sin\theta & \sin\left(\theta + \frac{8\pi}{5}\right) & \sin\left(\theta + \frac{6\pi}{5}\right) & \sin\left(\theta + \frac{4\pi}{5}\right) & \sin\left(\theta + \frac{2\pi}{5}\right) \\ \cos\theta & \cos\left(\theta + \frac{4\pi}{5}\right) & \cos\left(\theta + \frac{8\pi}{5}\right) & \cos\left(\theta + \frac{2\pi}{5}\right) & \cos\left(\theta + \frac{6\pi}{5}\right) \\ \sin\theta & \sin\left(\theta + \frac{4\pi}{5}\right) & \sin\left(\theta + \frac{8\pi}{5}\right) & \sin\left(\theta + \frac{2\pi}{5}\right) & \sin\left(\theta + \frac{8\pi}{5}\right) \\ \frac{1}{\sqrt{2}} & \frac{1}{\sqrt{2}} & \frac{1}{\sqrt{2}} & \frac{1}{\sqrt{2}} & \frac{1}{\sqrt{2}} \end{bmatrix} \begin{bmatrix} V_a \\ V_b \\ V_c \\ V_d \\ V_c \end{bmatrix} \tag{11}$$

completely decoupled from direct and quadrature axis components and vice-versa. These components have absent in rotor windings and zero sequence component also have deliberately absent by the short circuit of the rotor bars.

V. FABRICATION OF FPIM

Conventional 3-Φ squirrel cage motor has considered making the proposed FPIM. Considered 3-Φ motor has 24-slots, 4-poles stator and it is multiples of three as shown in Fig. 9. Proposed FPIM stator has required 20-solts, 2-poles and multiples of five. Remaining four slots (i.e., 1, 7, 13 and 19 slots) have left with no winding.

FIGURE 9. Components of conventional machine (3-Φ).

FPIM have deficiency of four slots the machine had run smoothly. Fig. 10 shows the FPIM stator winding arrangement and terminals are represented as a, b, c, d, and e respectively. Phase-a phase terminal is in 2nd slot and it is connected to 14th slot neutral terminal and 3rd slot winding connected to 15th slot winding then it is energized by the source. In the same way the phase-b, c, d, and e phase terminals and neutral terminals have connected accordingly.
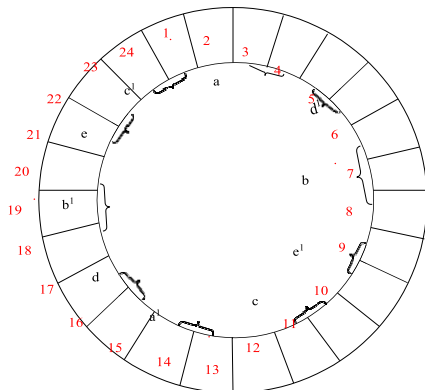
FIGURE 10. Winding slots of FPIM.

Winding connection diagram is shown in Fig. 11. This connection diagram clearly visualizes the slots connected for each other to achieve the required 5-Φ supply.
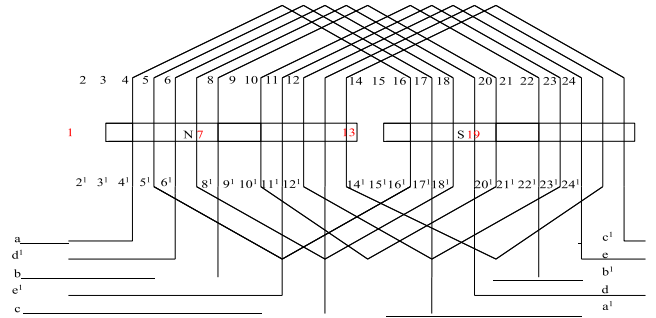
FIGURE 11. Winding diagram of FPIM.

After re-designed the 3-ΦIM into FPIM is shown in Fig. 12. The copper winding has rearranged and placed in respective slots with the help of winding diagram shown in Fig. 11.
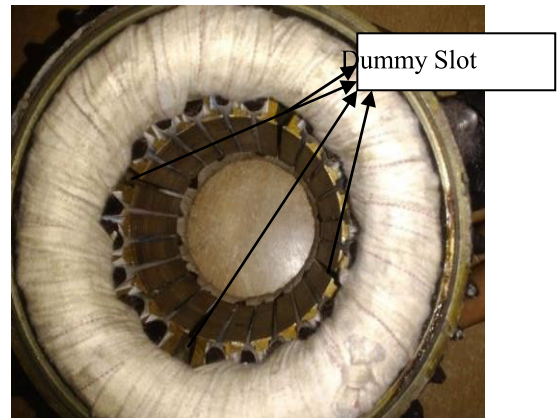
FIGURE 12. Slots with copper windings of FPIM.

FIGURE 13. Proposed transformer in Wye-Wye topology fed FPIM.

Proposed FPIM experimental setup has shown in Fig. 13. This experimental setup has 3-Φ to 5-Φ transformer, FPIM, watt meters, volt meters and ammeters etc. Fig. 14 has the instrument and it is used to measure the power factor, Torque and speed of FPIM in experimental setup.
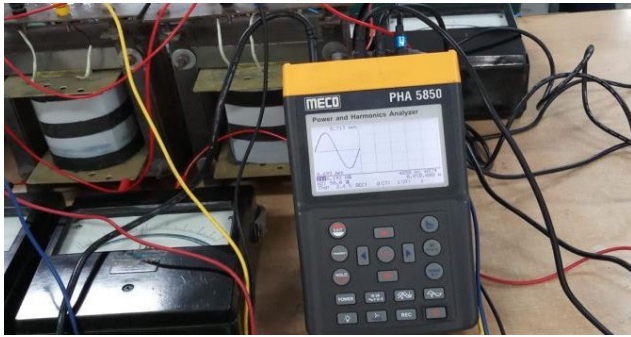
FIGURE 14. Measurement of power factor, torque and speed of the FPIM.

Proposed FPIM given best performance even one of the phases has failed and it is verified by the experimental setup. Fig. 15 depicts various phase loss scenarios under various conditions.

Case-1: Four phases like a, b, c & d are healthy and phase-e has phase loss, it has produced the pulsated torque nearly 13.8 N-m. It is shown in Fig. 15(i).

Case-2: Two adjcent phases like phase d & e have the phase loss, pulsated torque is nearly 13 N-m. It is shown in Fig. 15(ii).

Case-3: Three adjcent phases like c, d & e have phase loss, pulsated torque is nearly 12.8 N-m. It is shown in Fig. 15(iii).

Above mentioned phase loss conditions can explaine with respect to its steady state and transient response. From the observations the speed of the motor is almost constant. To operate for above rated speed based on field weakening condition and it has apllied to the proposed FPIM to observe the performance. The main observation is, once current has reduced to weakening the flux and speed of the motor increased above it's rated speed. So, the proposed FPIM is preferred for high speed applications. Same setup has observed in MATLAB-Simulink.

VI. RESULTS AND DISCUSSIONS

Proposed FPIM working/performance has analyzed with MATLAB-Simulink and with experimental setup. The obtained results are discussed and compared in this section. The block diagram of the proposed system is shown in Fig. 16.

A. SIMULATION RESULTS

Proposed FPIM fed by a Transformer Topology.

From the observation of MATLAB-Simulink results produced in Fig. 17 & 18, speed of the proposed FPIM is 2985 rpm and torque is 32 N-m. At 0.6 sec the torque has settled with value of 13.8 N-m. The same have obtained over experimental setup and tabulated in Table-2.

From Fig. 19, it is observed that 5-Φ starting currents are 8A (peak to peak) in all the phases for the 3 to 5-Φ transformer fed FPIM. The waveforms for three cycles are shown in Fig. 20.

(i)

(ii)

(iii)

FIGURE 15. FPIMD experimental setup under (i) One phase loss (ii) Two phase loss (iii) Three phase loss.
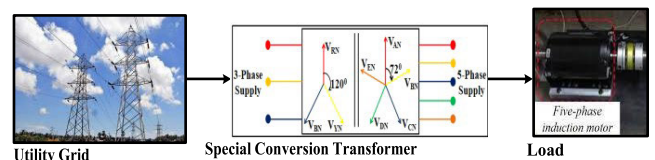
FIGURE 16. Block diagram of the proposed system.
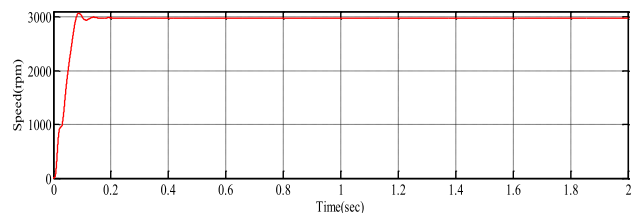
FIGURE 17. Speed of Transformer fed FPIMD under balanced condition.

From the Fig. 20, it is observed that input and output currents are 8 A and 4.2 A (peak to peak) of transformer in proposed system for three cycles respectively.
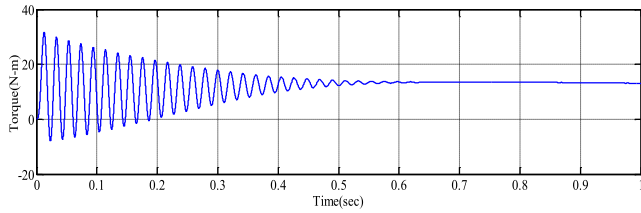
FIGURE 18. Torque of WYE-WYE Transformer FPIMD under balanced condition.
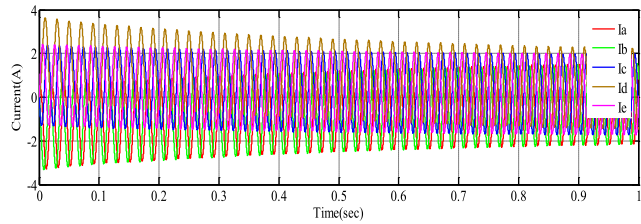
FIGURE 19. Starting currents of transformer fed FPIM in a balanced condition.
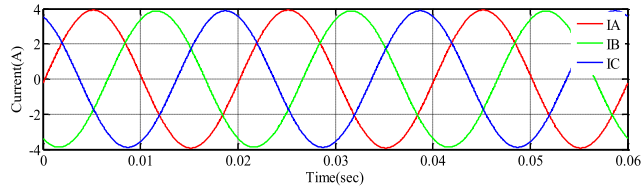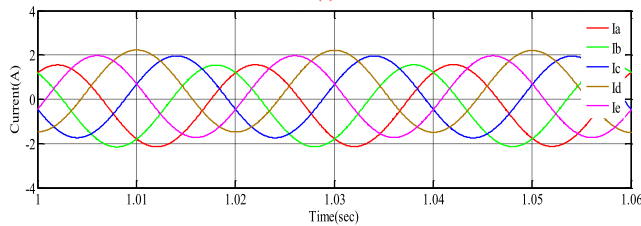
FIGURE 20. Currents of transformer fed FPIM under balanced condition (i) Input current of transformer (ii) Output current of transformer.

For the three cases of operation of proposed FPIM, it is observed that no changes at input and output voltages of transformer. There is slight change in speed and torque of the FPIM. The results have validated and tabulated which are through MATLAB-Simulink in Fig. 21 and through experimental setup in Table-2. In all above three cases, Torque has almost constant for the proposed FPIM.

It can be shown in Fig. 22 that under any phase loss circumstance, the stator currents have altered without the voltage changing. If there is only one phase of loss, or if the stator current $I_e = 0$, then the current is 2.6A. The stator currents $I_e = I_d = 0$, or the two phase loss condition, results in an output current of 2.6A. The magnitude of the output current is 4.1A under the three-phase loss condition, where the stator current $I_e = I_d = Ic = 0$.

The proposed FPIM has the better reliability and enhance all three phase loss conditions. However, several findings
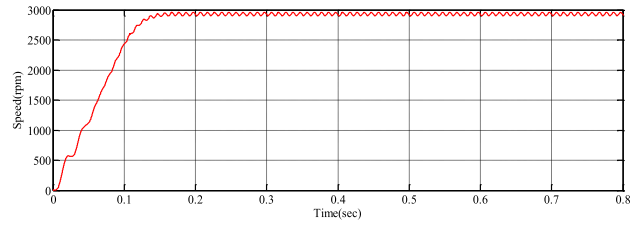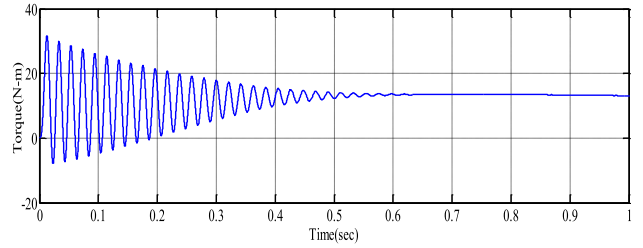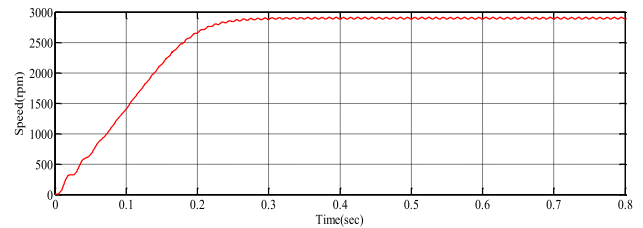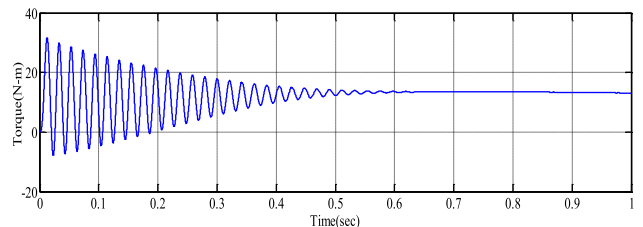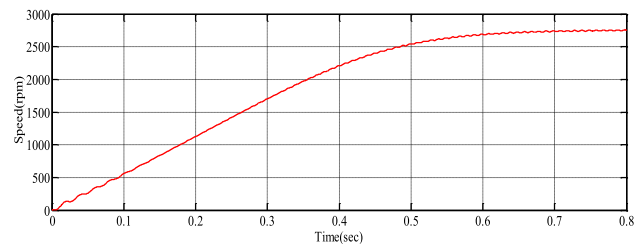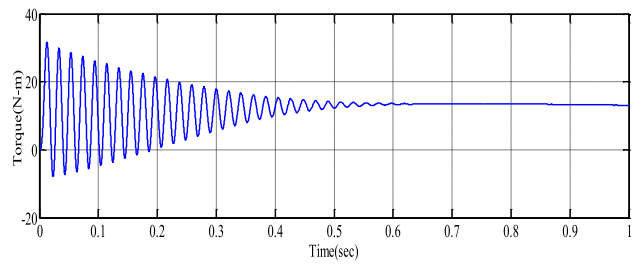
FIGURE 21. Speed and torque of transformer FPIM under one phase loss (ii) Two phase loss (iii) Three phase loss.

have been made, including that there hasn't been a change in voltages, the FPIM's performance hasn't really suffered, and stator currents have been adjusted appropriately.
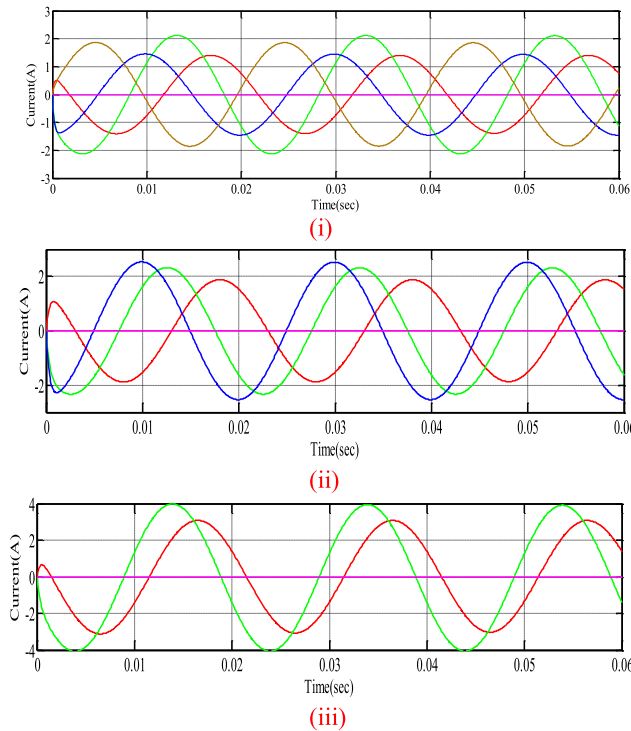
FIGURE 22. Stator Currents of Transformer FPIM under (i) one phase loss (ii) two phase loss (iii) three phase loss.

Similar type of analysis has done in different combinations like: Proposed Induction Motor Fed by a WYE-POLYGON Topology, Proposed Induction Motor Fed by a DELT - WYE Topology, Proposed Induction Motor Fed by a DELTA - POLYGON Topology and corresponding values have tabulated in Table 1.

TABLE 1. Starting and steady state torque of 3-Φ to 5-Φ transformer fed FPIM.

Topology	Starting Torque (Nm)	Setting Time	Steady State Torque (Nm)
Wye-Wye	32	0.6	13.8
Wye-Polygon	28	0.8	13.2
Delta-Wye	110	0.6	14.2
Delta- Polygon	68	0.7	13.8

From Table 1, starting and steady torques have been observed for all topologies of 3-Φ to 5-Φ transformer fed FPIM. Due to low peak overshoot of WYE-POLYGON transformer fed FPIM it gives the better performance at transient and steady state periods compared to other topologies.

B. EXPERIMENTAL RESULTS

Starting and steady state torque values are presented in Table 1. Input power (P_{in}) in watts, output power (P_{out}) in watts, speed in rpm, and torque in N-m values have obtained from experimental setup of FPIM are produced in Table 2.

TABLE 2. Input & output power, speed and torque of FPIMD.

Pin (W)	Pout (W)	Speed (rpm)	Torque (N-m)
5430	4320	2984	13.5

From Table 2, the speed and torque of the proposed FPIM experimental setup values are almost equal to MATLAB-Simulink setup values (from Fig. 15 & 16).

TABLE 3. Speed and torque under phase loss condition of FPIM.

No. of Φs loss	Speed (rpm)		Torque (N-m)	
	Simulation	Practical	Simulation	Practical
1	2980	2982	13.6	13.2
2	2972	2978	13.3	13
3	2944	2956	13.0	12.8

Experimental values and Simulation values of input and output current under phase loss condition of FPIM have tabulated in Table 4.

TABLE 4. Input and output currents of FPIMD under phase loss condition.

Simulation Results							
No. of Φ loss	$I_{in}(A)$			$I_{out}(A)$			
	I_A	I_B	I_C	I_a	I_b	I_c	I_d	I_e
1	3.6	3.4	3.4	2.0	1.8	1.8	2.2	0
2	3.1	2.8	3.0	2.0	2.6	2.4	0	0
3	4.0	3.8	3.7	4.1	3.2	0	0	0
Experimental Results							
No. of Φ loss	$I_{in}(A)$			$I_{out}(A)$			
	I_A	I_B	I_C	I_a	I_b	I_c	I_d	I_e
1	3.5	3.6	3.5	1.8	2.2	1.9	2	0
2	2.9	3.4	3.5	2.2	3.2	3.1	0	0
3	3.8	3.8	3.7	3.6	3.4	0	0	0

From Table 4, it can be shown that when phase loss occurs in the FPIM and both setup values are roughly identical, the stator currents increase.

TABLE 5. Comparison of the no load power factor and drive efficiency of 3-Φ and 5-Φ phase induction machines.

No. of Φ loss	3-Φ Induction Machine		5-Φ Induction Machine	
	Efficiency (%)	No-Load p.f.	Efficiency (%)	No-Load p.f
1	85	0.125	83	0.24
2	--	--	81	0.17
3	--	--	78	0.14

Table 5 displays the performance and no-load power factor of the 3-Φ and 5-Φ IM.

The suggested drive works even when one, two and three phases fail, so that the motor's performance is unaffected.

VII. CONCLUSION

The proposed FPIM has been found to be superior to 3-Φ IM. The basic functioning principle and torque production of FPIM are discussed. The dynamic performance of FPIM has been investigated using Park's transformation. The fabrication of 2 poles, 20 slot FPIM is combined with standard 3-Φ IM, 4 pole, 24 slot fabrication. All topologies of three to five phase transformers were tested using simulation using MATLAB/SIMULINK fed FPIM, and the results of 3 Φ to 5 Φ transformer fed FPIM were validated with prototypes for various phase loss circumstances. Constant torque is obtained in all topologies fed by FPIM, even with phase loss situations, such as 96% with one phase loss, 94% with two phase loss, and 90% with three phase loss. The efficiency and p.f achieved by FPIM is 1.92 times that of 3-Φ IM under one phase loss. The primary advantage of FPIM versus 3-Φ IM is that system performance remains unchanged even with a phase loss of two or three. Motor efficiency was observed to be 81% and 78% in both circumstances.

REFERENCES

[1] M. Walker, "The supply of single-phase power from three-phase systems," *J. Inst. Electr. Eng.*, vol. 57, no. 278, pp. 109–139, Jan. 1919.

[2] P. H. Chase, "Two-phase, five-wire distribution its engineering and economic elements," *Trans. Amer. Inst. Electr. Eng.*, vol. 44, pp. 737–749, Jan. 1925.

[3] E. Clarke, "Three-phase multiple-conductor circuits," *Trans. Amer. Inst. Electr. Eng.*, vol. 51, no. 3, pp. 809–821, Sep. 1932.

[4] E. E. Ward and H. Härer, "Preliminary investigation of an invertor-fed 5-phase induction motor," *Proc. Inst. Elect. Eng.*, vol. 116, no. 6, pp. 980–984, 1969.

[5] T. Kataoka, "A magnetic single-phase to 3-phase power converter and its characteristics," *IEEE Trans. Magn.*, vol. MAG-14, no. 5, pp. 999–1001, Sep. 1978.

[6] E. H. Badawy, M. K. El-Sherbiny, A. A. Ibrahim, and M. S. Farghaly, "A method of analyzing unsymmetrical faults on six-phase power systems," *IEEE Trans. Power Del.*, vol. 6, no. 3, pp. 1139–1145, Jul. 1991.

[7] L. Xu, "Rotor structure selections of nonsine five-phase synchronous reluctance machines for improved torque capability," *IEEE Trans. Ind. Appl.*, vol. 36, no. 4, pp. 1111–1117, Jul./Aug. 2000.

[8] E. Levi, M. Jones, S. N. Vukosavic, and H. A. Toliyat, "A novel concept of a multiphase, multimotor vector controlled drive system supplied from a single voltage source inverter," *IEEE Trans. Power Electron.*, vol. 19, no. 2, pp. 320–335, Mar. 2004.

[9] H. Nakra and T. Barton, "Three phase transformer transients," *IEEE Trans. Power App. Syst.*, vol. PAS-93, no. 6, pp. 1810–1819, Nov. 1974.

[10] B. S. Ram, J. A. C. Forrest, and G. W. Swift, "Effects of harmonics on converter transformer load losses," *IEEE Trans. Power Del.*, vol. 3, no. 3, pp. 1059–1066, Jul. 1988.

[11] C. M. Arturi, "Transient simulation and analysis of a three-phase five-limb step-up transformer following an out-of-phase synchronization," *IEEE Trans. Power Del.*, vol. 6, no. 1, pp. 196–207, Jan. 1991.

[12] A. Rezaei-Zare, "Enhanced transformer model for low- and mid-frequency transients—Part II: Validation and simulation results," *IEEE Trans. Power Del.*, vol. 30, no. 1, pp. 316–325, Feb. 2015.

[13] A. Tripathi and G. Narayanan, "Evaluation and minimization of low-order harmonic torque in low-switching-frequency inverter-fed induction motor drives," *IEEE Trans. Ind. Appl.*, vol. 52, no. 2, pp. 1477–1488, Mar. 2016.

[14] Y. Mei, S. Wang, and X. Zhang, "A model predictive torque control method for dual induction motor drive system fed by indirect matrix converter," in *Proc. IEEE 8th Int. Power Electron. Motion Control Conf. (IPEMC-ECCE Asia)*, May 2016, pp. 2837–2841.

[15] V. M. Sundaram and H. A. Toliyat, "Stator inter-turn fault detection for seamless fault-tolerant operation of five-phase induction motors," in *Proc. IEEE Energy Convers. Congr. Expo. (ECCE)*, Sep. 2016, pp. 1–8.

[16] J. Listwan and K. Pieńkowski, "Control of five-phase induction motor with application of second-order sliding-mode direct field-oriented method," in *Proc. Int. Symp. Electr. Mach. (SME)*, Jun. 2017, pp. 1–6.

[17] Y. N. Tatte, M. V. Aware, J. Pandit, and R. Nemade, "Performance improvement of three-level five-phase inverter fed DTC controlled five-phase induction motor during low-speed operation," in *Proc. IEEE Int. Conf. Power Electron., Drives Energy Syst. (PEDES)*, Dec. 2016, pp. 1–6.

[18] A. S. Ananda and C. P. Manjesh, "Evaluation of harmonic and THD using LC filter for five phase induction motor drive at low speed," in *Proc. Int. Conf. Circuit, Power Comput. Technol. (ICCPCT)*, Apr. 2017, pp. 1–4.

[19] M. I. Masoud, A. S. Abdelkhalik, and R. Al-Abri, "Vector controlled five-phase PWM-CSI induction motor drive fed from controlled three-phase PWM current source rectifier," in *Proc. 7th IET Int. Conf. Power Electron., Mach. Drives (PEMD)*, Apr. 2014, pp. 1–6.

[20] S. Lu and K. Corzine, "Direct torque control of five-phase induction motor using space vector modulation with harmonics elimination and optimal switching sequence," in *Proc. 21st Annu. IEEE Appl. Power Electron. Conf. Expo. (APEC)*, Mar. 2006, p. 7.

[21] J. Du, G. Mo, G. Wu, and K. Huang, "An improved method for induction motor constant current soft-starting using fuzzy-control," in *Proc. 6th Int. Conf. Fuzzy Syst. Knowl. Discovery*, vol. 4, Aug. 2009, pp. 52–56.

[22] F. Hamidia, A. Abbadi, and M. Boucherit, "Direct torque controlled dual star induction motors (in open and closed loop)," in *Proc. 4th Int. Conf. Electr. Eng. (ICEE)*, Dec. 2015, pp. 1–6.

[23] B. V. Reddy and V. T. Somasekhar, "An SVPWM scheme for the suppression of zero-sequence current in a four-level open-end winding induction motor drive with NestedRectifier–inverter," *IEEE Trans. Ind. Electron.*, vol. 63, no. 5, pp. 2803–2812, May 2016.

[24] P. Gopi, P. S. Varma, C. N. S. Kalyan, C. V. Ravikumar, A. Srinivasulu, B. Bohara, A. Rajesh, M. N. B. A. Wahab, and K. Sathish, "Dynamic behavior and stability analysis of automatic voltage regulator with parameter uncertainty," *Int. Trans. Electr. Energy Syst.*, vol. 2023, Jan. 2023, Art. no. 6662355, doi: 10.1155/2023/6662355.

P. SRINIVASA VARMA (Senior Member, IEEE) received the B.Tech. degree from JNTUH, the M.Tech. degree from the JNTUA College of Engineering, Ananthapuramu, and the Ph.D. degree from JNTU Anantapur. He is currently an Associate Professor with the EEE Department, K. L. University, Guntur, Andhra Pradesh. He is also an Associate Dean of Research and Development with the Koneru Lakshmaiah Education Foundation. He has published 72 research papers in various international journals and conferences. He has published 12 Indian patents.

K. P. PRASAD RAO (Member, IEEE) received the M.Tech. degree in power systems and power electronics from Acharya Nagarjuna University, Guntur, in 2010, and the Ph.D. degree in power systems from K. L. Deemed to be University, Guntur, in 2021.

He is currently a Professor with the Department of Electrical and Electronics Engineering, Narayana Engineering College, Gudur. His current research interests include multiphase power system and power electronics, and AI technology in electrical systems.

C. V. RAVIKUMAR received the M.Tech. degree in digital electronics and communication system from Jawaharlal Nehru Technology University, Anantapur, in 2009, and the Ph.D. degree in communication networks from the Vellore Institute of Technology (VIT) Vellore, India, in 2018. He is currently an Assistant Professor SG with the School of Electronics Engineering, Department of Embedded Technology, VIT Vellore. His current research interests include communication networks, machine learning, deep learning, wireless sensor networks, and information security.

K. SATHISH received the master's degree in communication systems from Jawaharlal Nehru Technology University, Anantapur, India, in 2017. He is currently a Research Scholar with the School of Electronics Engineering, Vellore Institute of Technology, Vellore, Tamil Nadu, India. His research interests include underwater wireless sensor networks, 5G communications, machine learning, and artificial intelligence.

GIOVANNI PAU (Member, IEEE) received the bachelor's degree in telematic engineering from the University of Catania, Italy, and the master's (cum laude) and Ph.D. degrees in telematic engineering from Kore University of Enna, Italy. He is currently an Associate Professor with the Faculty of Engineering and Architecture, Kore University of Enna. He is the author/coauthor of more than 80 refereed articles published in journals and conference proceedings. His research interests include wireless sensor networks, fuzzy logic controllers, intelligent transportation systems, the Internet of Things, smart homes, and network security. He has been involved in several international conferences as the session co-chair and a technical program committee member. He serves/served as a leading guest editor for special issues of several international journals. He is an Editorial Board Member and an Associate Editor of several journals, such as IEEE AccEss, *Wireless Networks* (Springer), *EURASIP Journal on Wireless Communications and Networking* (Springer), *Wireless Communications and Mobile Computing* (Hindawi), *Sensors* (MDPI), and *Future Internet* (MDPI), to name a few.

RAJEEV PANKAJ NELAPATI (Senior Member, IEEE) received the B.E. degree in electronics and communication engineering from the Andhra University College of Engineering, Vishakhapatnam, India, in 2006, the M.Tech. degree in VLSI design from the Indian Institute of Technology Guwahati, Guwahati, in 2009, and the Ph.D. degree from the Vellore Institute of Technology (VIT), Vellore, India, in 2019. From 2009 to 2022, he was an Assistant Professor with the Department of Micro and Nanoelectronics, VIT. Since 2023, he has been an Assistant Professor Senior with VIT. He is the author for more than ten articles in reputed international journals. His research interests include TCAD modeling of nanostructures, bio-sensors, neuromorphic circuits, and machine learning in VLSI.

● ● ●